

# Spin Reorientation Studies in $\text{Nd}_2\text{Fe}_{14-x}\text{Si}_x\text{B}$ ( $0 < x \leq 2$ )

R. GARGULA, A.T. PEŃDZIWIATR, B.F. BOGACZ, S. WRÓBEL

Institute of Physics, Jagiellonian University  
Reymonta 4, 30-059 Cracow, Poland

J. BARTOLOMÉ AND J. STANKIEWICZ

Faculty of Science, University of Zaragoza – CSIC, 50009 Zaragoza, Spain

*(Received November 2, 2001)*

$\text{Nd}_2\text{Fe}_{14-x}\text{Si}_x\text{B}$  ( $x = 0.25, 0.5, 0.75, 1.0, 1.5, 2.0$ ) intermetallic compounds were investigated by magnetometry,  $^{57}\text{Fe}$  Mössbauer effect, electric resistivity, and differential scanning calorimetry mainly in the vicinity of the spin reorientation temperature,  $T_{\text{SR}}$ . The Curie temperature,  $T_{\text{C}}$ , and  $T_{\text{SR}}$  were determined for different compositions and the spin phase diagram was constructed.  $^{57}\text{Fe}$  Mössbauer spectra showed noticeable changes in the reorientation region. For temperatures above the transition, the spectra were analysed using 6 Zeeman patterns associated with 6 inequivalent crystal sites in  $\text{Nd}_2\text{Fe}_{14}\text{B}$  according to site occupations ( $16k_1:16k_2:8j_1:8j_2:4c:4e$ ). In the transition region, 12 subspectra had to be incorporated in the analysis. Electric resistivity measurements showed a typical metallic behaviour with no anomalies in the magnetic transition region. Differential scanning calorimetry measurements revealed broad endothermic two stage peaks around  $T_{\text{SR}}$ .

PACS numbers: 75.50.Ww, 76.80.+y, 64.60.-i

## 1. Introduction

$\text{Nd}_2\text{Fe}_{14}\text{B}$  is now the leading material for permanent magnet applications. The  $\text{Nd}_2\text{Fe}_{14}\text{B}$  type compounds crystallise in a tetragonal structure with space group  $P4_2/mnm$  [1]. Iron atoms occupy six non-equivalent crystal sites ( $16k_1$ ,  $16k_2$ ,  $8j_1$ ,  $8j_2$ ,  $4e$ ,  $4c$ ), the rare-earth ions occupy  $4f$  and  $4g$  crystallographic sites and boron is located at  $4g$  site [2]. Silicon substitution into this compound causes a

slight increase in the Curie temperature and brings changes in the spin reorientation phenomenon observed in  $\text{Nd}_2\text{Fe}_{14}\text{B}$  around 130 K [3]. This magnetic transition is from conical spin arrangement (spins tilted from crystallographic  $c$ -axis below  $T_{\text{SR}}$ ) to axial spin arrangement (spins aligned along  $c$ -axis above  $T_{\text{SR}}$ ).

Neutron-diffraction study of  $\text{Nd}_2\text{Fe}_{14-x}\text{Si}_x\text{B}$  showed that silicon exhibits a strong preference for the iron 4c sites, a moderate preference for the 8j<sub>1</sub> site, is almost excluded from the 16k<sub>2</sub> site, and is totally excluded from the 8j<sub>2</sub>, 16k<sub>1</sub>, and 4e sites [4]. Silicon site occupations were studied also by  $^{57}\text{Fe}$  Mössbauer spectroscopy [5, 6].

In our study,  $\text{Nd}_2\text{Fe}_{14-x}\text{Si}_x\text{B}$  ( $x = 0.25, 0.5, 0.75, 1.0, 1.5, 2.0$ ) compounds have been investigated by magnetometry,  $^{57}\text{Fe}$  Mössbauer effect, electric resistivity, and differential scanning calorimetry (DSC) to establish the influence of silicon on the spin reorientation phenomenon. Our main goal was to determine the spin phase diagram, the temperature span of the magnetic transition and the influence of this transition on hyperfine interaction parameters, as well as to study the thermal effect connected with the transition.

## 2. Experimental

$\text{Nd}_2\text{Fe}_{14-x}\text{Si}_x\text{B}$  compounds were produced by a standard procedure of the induction melting under flowing high purity argon and the subsequent annealing at 900°C for two weeks. In the case of iron substitution by silicon up to  $x = 2.0$ , the X-ray and thermomagnetic analysis showed the presence of only one phase. For higher silicon content  $x \geq 2.5$  a mixture of phases has been observed. However, the Mössbauer spectra indicated a small amount of natural iron impurity (about 2%) for  $\text{Nd}_2\text{Fe}_{14-x}\text{Si}_x\text{B}$ ,  $x = 0.5, 1.5$  compounds. These impurity patterns were subtracted from the experimental spectra by a numerical procedure. Magnetic measurements were performed using a SQUID magnetometer from the temperature 4.2 K to 300 K and by using a Faraday-type balance in the temperature range 300–770 K. The ac-electrical resistivity measurements were performed with a six-probe method on bar-shaped samples in the temperature range 4.2 K to 300 K.  $^{57}\text{Fe}$  Mössbauer transmission spectra were recorded from liquid nitrogen temperature to room temperature using a  $^{57}\text{Co}(\text{Rh})$  source and a computer driven constant acceleration mode spectrometer. The spin reorientation transition has been studied extensively by narrow step temperature scanning in the reorientation region. A high purity metallic iron foil was used to calibrate the velocity scale. Isomer shifts were given with respect to the centre of gravity of the room temperature iron Mössbauer spectrum. Two samples of  $\text{Nd}_2\text{Fe}_{14-x}\text{Si}_x\text{B}$ ,  $x = 0.25, 0.5$  have been studied also by DSC in the temperature range 165–295 K. The measurements were performed in heating and cooling cycles at different scanning rates.

### 3. Results and discussion

The spin reorientation and Curie temperatures determined from magnetic measurements were used to construct the spin phase diagram (Fig. 1). Silicon substitution into  $\text{Nd}_2\text{Fe}_{14}\text{B}$  causes an increase in the Curie temperature and a decrease in spin reorientation temperature so the conical spin structure region is getting smaller upon Si substitution.

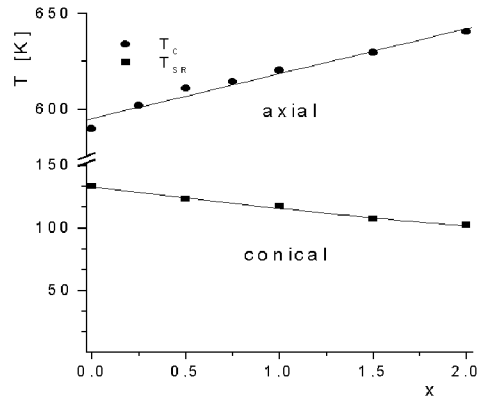


Fig. 1. Spin structure phase diagram for  $\text{Nd}_2\text{Fe}_{14-x}\text{Si}_x\text{B}$  system.

Electrical resistivity measurements of  $\text{Nd}_2\text{Fe}_{14-x}\text{Si}_x\text{B}$  ( $x = 0.0$  [7], 0.5, 1.5, 2.0) were performed in the range from 4.2 K to 300 K. The behaviour is typical of metallic compounds, no anomalies were observed in the transition region. Applying Matthiessen's rule, the total resistivity can be written as [7]:

$$\rho = \rho_0 + \rho_{\text{ph}} + \rho_{\text{mag}}, \quad (1)$$

where  $\rho_0$  is the temperature independent residual resistivity,  $\rho_{\text{ph}}$  is the resistivity arising from electron-phonon scattering and  $\rho_{\text{mag}}$  is the magnetic (spin) resistivity, respectively.  $\rho_0$  increases from  $5 \mu\Omega \text{ cm}$  (for  $x = 0$ ) to  $168 \mu\Omega \text{ cm}$  (for  $x = 2$ ) upon Si substitution. Changes in  $\rho_0$  may be due to the lower number of conduction electrons carried by Si atoms than by Fe atoms and to the disorder introduced by the Si substitution.

Selected Mössbauer spectra for the  $\text{Nd}_2\text{Fe}_{13.5}\text{Si}_{0.5}\text{B}$  intermetallic compound are shown in Fig. 2. The Lorentzian approximation was used to describe the line shape of the Mössbauer spectra. A simultaneous fitting of several Mössbauer spectra gave opportunity to establish consistent description of all spectra and the temperature dependence of hyperfine interaction parameters. The spectra above the region of spin reorientation were analysed using six Zeeman subspectra corresponding to the six crystallographically distinct sites. The relative areas of the sextets were taken from the silicon occupation data obtained from the neutron diffraction results, given in [4]. Each subspectrum was characterised by the following hyperfine

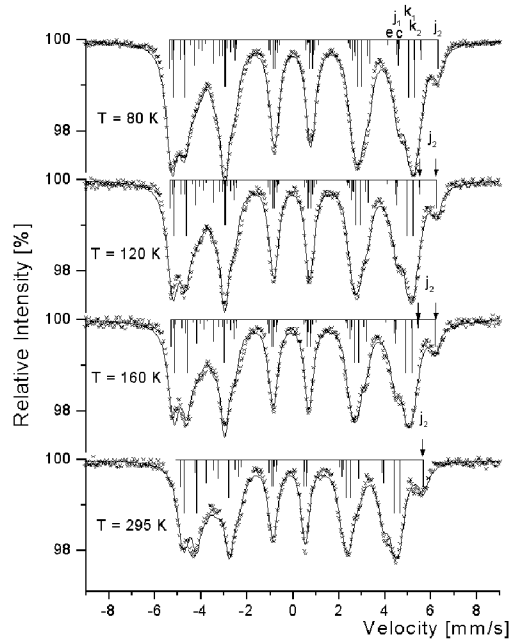


Fig. 2. Selected  $^{57}\text{Fe}$  Mössbauer transmission spectra for the  $\text{Nd}_2\text{Fe}_{14-x}\text{Si}_x\text{B}$  ( $x = 0.5$ ) intermetallic compound. The solid lines are fits to the data. The stick diagrams show the line positions and relative intensities. Positions of the sixth line of  $8j_2$  sextets are specially marked. In the transition region  $8j_2$  has two positions, corresponding to “low” and “high temperature” Zeeman sextets, marked by arrows.

interaction parameters: magnetic field,  $H$ , isomer shift,  $IS$ , quadrupole splitting,  $QS$  (defined as  $[(V_6 - V_5) - (V_2 - V_1)]$ , where  $V_i$  are velocities corresponding to Mössbauer line positions from the left to the right).

The amplitude of the sixth, separated line of the  $8j_2$  sublattice Zeeman sextet (Fig. 2) which changes its value with increasing temperature in the transition region is the result of the splitting of  $8j_2$  Zeeman sextet into two parts, in a similar manner as described for  $\text{Er}_2\text{Fe}_{14}\text{B}$  compound [8]. In this description it was assumed that there is a coexistence of the “low” and “high temperature” Zeeman sextets in the transition region. The “low temperature” sextets describe the spectra in temperatures below the transition while the “high temperature” sextets describe the spectra above the transition. In the spin reorientation region the “low” and the “high temperature” Zeeman sextets exchange gradually (between themselves) their contributions  $C_l$  and  $C_h$  to the total spectrum. Temperature dependencies of subspectra contributions  $C_l$ ,  $C_h$  of both kinds of Zeeman sextets are shown in Fig. 3. From this plot we derived the temperature span of spin reorientation to be 90–160 K.

In the region of transition the “low” and “high temperature” Zeeman sextets have different values of  $H$  and  $QS$ . In the description of spectra, the weak,

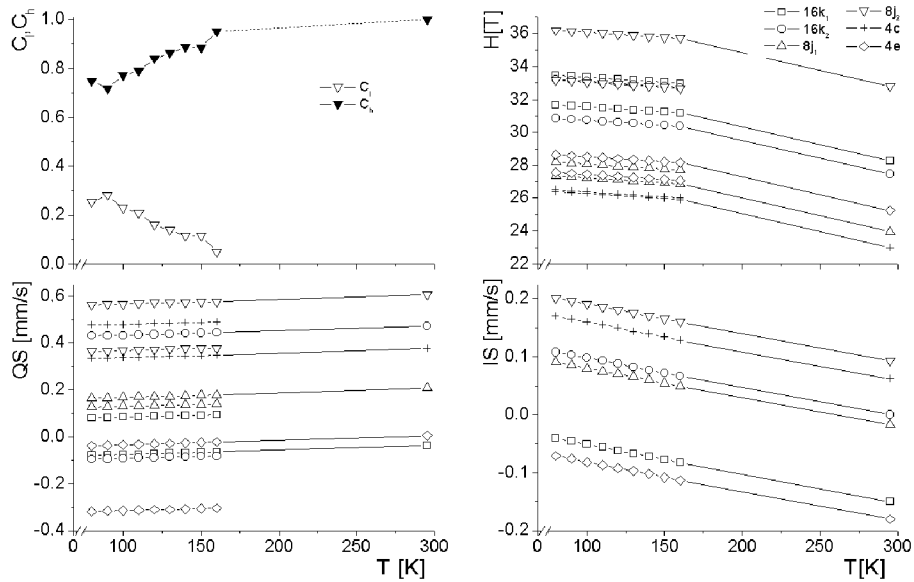


Fig. 3. Temperature dependencies of subspectra contributions for both  $C_1$  — “low temperature” (open triangle) and  $C_h$  — “high temperature” (solid triangle) Zeeman sextets and temperature dependencies of hyperfine parameters:  $H$ ,  $QS$ ,  $IS$  for  $\text{Nd}_2\text{Fe}_{14-x}\text{Si}_x\text{B}$ ,  $x = 0.5$ . The average errors are  $H(0.1 \text{ T})$ ,  $QS(0.01 \text{ mm/s})$ ,  $IS(0.01 \text{ mm/s})$ .

systematic changes of  $H$  and  $QS$  with temperature were taken into account. Also a common linear dependence of  $IS$  (Fig. 3), caused by second-order Doppler shift effect was assumed for “high” and “low temperature” Zeeman sextets.

The temperature dependencies of the hyperfine magnetic field derived from the spectra are shown in Fig. 3. The attribution of  $H$  to the crystal sublattices was based on the nearest neighbours argumentation [2]. The hyperfine magnetic field decreases with the increase in temperature for all sublattices. The behaviour of  $QS$  is connected with the change of angle between the easy axis of magnetisation and the electric field gradient [9].  $QS$  parameters are temperature independent for all sublattices.

The DSC measurements of  $\text{Nd}_2\text{Fe}_{14-x}\text{Si}_x\text{B}$ ,  $x = 0.5$ , were performed in heating and cooling cycles at different scanning rates. The best results were obtained in scans with the rate of 50 K/min. In Fig. 4 there are shown the heat flow anomalies accompanying the spin reorientation from conical to axial spin arrangement (upper curve) with increasing temperature for  $\text{Nd}_2\text{Fe}_{14-x}\text{Si}_x\text{B}$ ,  $x = 0.5$ . The endothermic (heating) and exothermic (cooling) changes have the character of two stage anomalies. Earlier DSC study of the similar system  $\text{Nd}_2(\text{Fe}_{1-x}\text{Co}_x)_{14}\text{B}$ ,  $x = 0, 0.1$  [10] also reports the endothermic transition due to spin reorientation.

In this type of spin reorientation transition it is difficult to establish the spin reorientation temperature from DSC data. Only the span of spin reorienta-

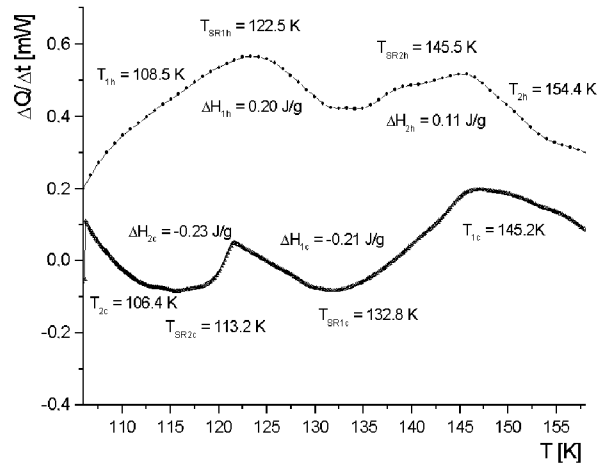


Fig. 4. Endothermic transition due to spin reorientation measured by differential scanning calorimetry for the  $\text{Nd}_2\text{Fe}_{14-x}\text{Si}_x\text{B}$ ,  $x = 0.5$  compound. Upper and lower curves show results of measurements, which were performed on heating (h indexes) and cooling (c indexes), respectively, both at rate 50 K/min.  $T_1$  and  $T_2$  are the temperatures taken as the onset and the end of peak, respectively.

tion transition was estimated to be 45 K, from 105 K to 150 K. From calorimetric measurements the enthalpy of transition was estimated to be  $\Delta H = (0.37 \pm 0.07)$  J/g. The same type of anomalies were detected for sample  $x = 0.25$ .

### References

- [1] J.F. Herbst, J.J. Croat, F.E. Pinkerton, W.B. Yelon, *Phys. Rev. B* **29**, 4176 (1984).
- [2] G.J. Long, F. Grandjean, in: *Supermagnets — Hard Magnetic Materials, NATO ASI Series Conf., II Ciocco (Italy) 1990*, Ed. G.J. Long, NATO ASI, II Ciocco (Italy) 1990, p. 23.1.
- [3] A.T. Pedziwiatr, E.W. Wallace, E. Burzo, *IEEE Trans. Magn.* **MAG-23**, 1795 (1987).
- [4] G.K. Marasinghe, O.A. Pringle, G.J. Long, W.J. James, D. Xie, J. Li, W.B. Yelon, F. Grandjean, *J. Appl. Phys.* **74**, 6798 (1993).
- [5] Z.W. Li, X.Z. Zhou, A.H. Morrish, *Phys. Rev. B* **41**, 8617 (1990).
- [6] A. Kowalczyk, P. Stefański, M. Budzyński, *Phys. Status Solidi A* **139**, K121 (1993).
- [7] J. Stankiewicz, J. Bartolomé, *Phys. Rev. B* **55**, 3058 (1997).
- [8] R. Wielgosz, A.T. Pędziwiatr, B.F. Bogacz, S. Wróbel, *Mol. Phys. Rep.* **30**, 167 (2000).
- [9] P. Gütlich, R. Link, A. Trautwein, *Mössbauer Spectroscopy and Transition Metal Chemistry*, Springer-Verlag, Berlin 1978, p. 28.
- [10] C.D. Fuerst, J.F. Herbst, E.A. Alson, *J. Magn. Magn. Mater.* **54-57**, 567 (1986).